

Dalton Transactions

Accepted Manuscript



This is an *Accepted Manuscript*, which has been through the Royal Society of Chemistry peer review process and has been accepted for publication.

Accepted Manuscripts are published online shortly after acceptance, before technical editing, formatting and proof reading. Using this free service, authors can make their results available to the community, in citable form, before we publish the edited article. We will replace this *Accepted Manuscript* with the edited and formatted *Advance Article* as soon as it is available.

You can find more information about *Accepted Manuscripts* in the [Information for Authors](#).

Please note that technical editing may introduce minor changes to the text and/or graphics, which may alter content. The journal's standard [Terms & Conditions](#) and the [Ethical guidelines](#) still apply. In no event shall the Royal Society of Chemistry be held responsible for any errors or omissions in this *Accepted Manuscript* or any consequences arising from the use of any information it contains.

Synthesis and properties of mono- and dimetal Fischer multicarbene complexes derived from thiophene and thieno[2,3-*b*]thiophene

Zandria Lamprecht, Nina A. van Jaarsveld, Daniela I. Bezuidenhout, David C. Liles and Simon Lotz.*

Department of Chemistry, University of Pretoria, Private Bag X20, Hatfield 0028, Pretoria, South Africa.

Abstract

Access to multicarbene complexes of a fused thienothiophene substrate was obtained by the use of the tetrabrominated thieno[2,3-*b*]thiophene precursor in a lithium-bromide exchange reaction, followed by nucleophilic attack on metal hexacarbonyls (M = Cr, W). Subsequent alkylation afforded unique triscarbene complexes $[M(CO)_4\{C(OEt)\}_2C_6H_4S_2C(OEt)M(CO)_5]$ (M = Cr **12**, W **13**) featuring three non-equivalent carbene ligands on a single thiophene linker, as well as the bischelated tetracarbene complexes $[M(CO)_4\{C(OEt)\}_2C_6S_2\{C(OEt)\}_2M(CO)_4]$ (M = Cr **14**, W **15**). The triscarbene complexes **12** and **13** are the first examples of multi-alkoxycarbene complexes featuring three non-equivalent carbene ligands. The reaction also afforded the chelated mononuclear biscarbene complexes $[M(CO)_4\{C(OEt)\}_2C_6H_2S_2]$ (M = Cr **10**, W **11**) in low yields. Similarly, employing tetrabromothiophene as precursor yielded the mononuclear chelate biscarbene complexes $[M(CO)_4\{C(OEt)\}_2C_4H_4S]$ (M = Cr **6**, W **7**) and the dinuclear tetracarbene complexes $[M(CO)_4\{C(OEt)\}_2C_4S\{C(OEt)\}_2M(CO)_4]$ (M = Cr **8**, W **9**). Modification of the classic Fischer carbene synthetic methodology to a process of stepwise additions of lithiating agent and metal carbonyls to thieno[2,3-*b*]thiophene, facilitates the formation of the mixed metal biscarbene complex $[W(CO)_5C(OEt)\{C_6H_2S_2\}C(OEt)Cr(CO)_5]$ **5**, as analogue of the homonuclear biscarbene complexes $[M(CO)_5C(OEt)\{C_6H_2S_2\}C(OEt)M(CO)_5]$, (M = Cr **3**, W **4**). The monocarbene complexes $[M(CO)_5\{C(OEt)\}_2C_6H_3S_2]$, (M = Cr **1**, W **2**) were also obtained in high yields, and the molecular structures of the tungsten complexes, with the exception of **9** and **11**, were confirmed by single crystal X-ray diffraction studies.

Introduction

The application of Fischer carbene complexes as template functionalities in organic chemistry is well studied and exploited.¹ Literature on the synthesis and reactivity of Fischer carbene complexes often reports a series of similar substrates to prepare classical monocarbene complexes, but the approach neglects the possibilities that a single substrate has to offer in multiple carbene complex synthesis. Although N-heterocyclic carbene complexes have found extensive application in multiple carbene functionalities on single substrates,² a similar strategy has not been developed in the chemistry of classic heteroatom-stabilized Fischer carbene complex-types. One way to increase the number of carbene ligands on a single substrate entails the synthesis of biscarbene complexes by sequential or dilithiation of a suitable substrate or by chelate formation.³ The preparation of a mononuclear bisalkoxycarbene chelate is challenging because the Fischer procedure requires a 1,2-dianion on the substrate during the synthesis. The proximity problem of dianions in benzene and olefins has been addressed previously by the successful preparation of the first examples of symmetrically substituted biscarbene chelates (Figure 1, **A**).³ Dötz and co-workers prepared analogous biscarbene chelates from N,N'-diphenylhydrazine.⁴ Recently we prepared the first examples of asymmetric bisalkoxycarbene complexes with two carbene ligands in electronically different environments and were surprised to find that the compounds were of relatively high stability. Examples of such chelating biscarbene complexes attached to a thiophene backbone are shown in Figure 1 (**B** and **C**).⁵ Chelation in **B** occurs as a result of the steric and electronic properties of the fused N-methylpyrrole ring, which

blocks one side of a thiophene ring and renders the β -proton of the thiophene ring comparable in acidity to the α -proton of the pyrrole ring. Hence, the second deprotonation can occur at either the α -position to the nitrogen atom or at the 3-position of the thiophene ring as both the chelate and biscarbene complexes have been isolated from the same reaction. In **C**, the desired chelation reaction could only be achieved after careful selection of the thiophene substrate. In 2-methyl-4-bromothiophene, a methyl substituent blocks one of the reactive α -positions while the bromo-substituent activates the 4-position to accommodate the lithium-bromine exchange reaction and facilitates chelation.

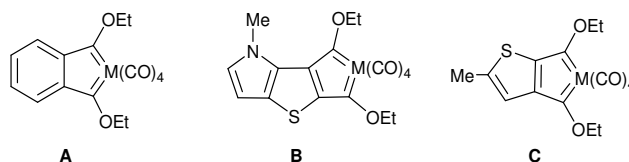
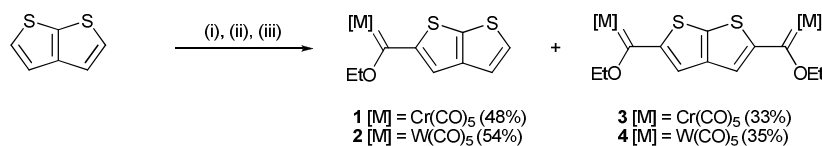


Figure 1: Examples of mononuclear biscarbene chelates.

The interest in heteroaromatic sulphur-containing ring systems lies in their electron excessive and planar properties which are transferable to long chain oligo- and polythiophenes, leading to exceptional charge transfer and conductivity in these compounds.⁶ The thiophene units in linear α -substituted chains (bithiophene or polythiophenes) tend to retain the thiophene characteristics with regard to proton acidities or even amplify them (charge transfer). In comparison, the planar complexes consisting of fused thiophene rings have a more rigid structure resulting in better overlap of p_{π} -orbitals and therefore show even more efficient π -resonance effects.⁷ Condensed thienyl rings retain optoelectronic and semiconducting properties but allow for the introduction of other characteristics. These molecules display higher voltage electronic band gaps and greater stability when compared to α -oligothiophenes. Unlike the chain structured thiophenes,⁸ annulated thiophenes are rather unexplored when it comes to their organometallic chemistry.⁹ The electron-withdrawing properties of the attached Fischer carbene moieties in combination with the charge transfer properties of thiophenes, hold great promise for potential application in this fast growing area of electronic and photonic thiophene materials. We report herein the syntheses of thieno[2,3-*b*]thiophene chelates and compare their spectral properties and structural features with the thiophene analogues. This work forms part of an ongoing study of the chemistry of multicarbene and multimetal-carbene complexes.¹⁰

Results and discussion

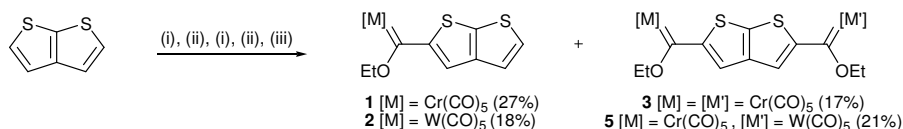
Thiophene and thieno[2,3-*b*]thiophene are commercially available but the latter can be synthesized from trimethylsilyl-1,3-pentadiyne,¹¹ which in turn is accessible from 1,4-bis(trimethylsilyl)-1,3-butadiyne.¹² Utilizing the most common Fischer method for the synthesis of metal-carbene complexes, different classes of Fischer carbene complexes could be prepared in this study. Commonly an anionic substrate reacts as a nucleophile with a carbonyl ligand of a neutral metal carbonyl precursor to form a metal acylate. After subsequent alkylation with an appropriate alkylating agent, the neutral Fischer carbene complex is generated. Thiophene and thieno[2,3-*b*]thiophene were selected as substrates for the lithiations. The first lithiation (deprotonation) occurs at the most acidic protons α to the sulfur atoms while the lithium-halogen exchange reactions will readily include β -positions. The mono- and biscarbene complexes, $[M(CO)_5\{C(OEt)C_6H_3S_2\}]$ ($M = Cr$ **1**, W **2**) and $[M(CO)_5C(OEt)\{C_6H_2S_2\}C(OEt)M(CO)_5]$ ($M = Cr$ **3**, W **4**), could be prepared in good yields using this method (Scheme 1), whereas the synthesis of the corresponding mon- and biscarbene complexes of thiophene have been reported earlier.⁵



Scheme 1: Synthesis of mono- and biscarbene complexes of thieno[2,3-*b*]thiophene. (i) 1.5 eq *n*-BuLi, (ii) 1.5 eq Cr(CO)₆ or W(CO)₆ (iii) excess [Et₃O][BF₄].

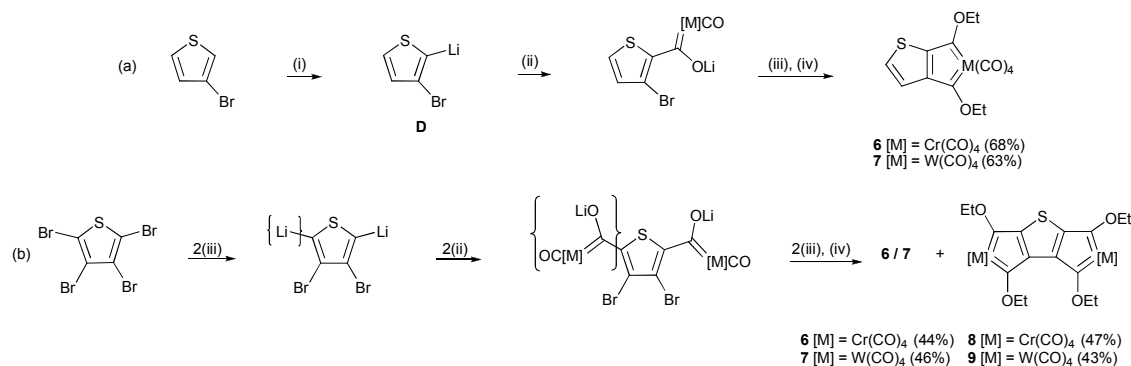
The addition of 1.5 equivalents of *n*-BuLi for each equivalent of thieno[2,3-*b*]thiophene was used to optimize the projected yields of the mono- and dilithiated thieno[2,3-*b*]thiophene, simultaneously obtaining both mono- and biscarbene products from the same reaction mixture. After the formation of the lithiated intermediates they were reacted with 1.5 equivalents of chromium or tungsten hexacarbonyl, and alkylation with excess triethyloxonium salt to afford the target products. Products were purified with column chromatography with an overall yield of 80–90% of **1–4**, Scheme 1. The biscarbene complexes of thieno[2,3-*b*]thiophene (**3**, **4**) display greater stability in solution (reactivity towards carbene oxidation) compared to analogous thiophene and linearly arranged thiophene biscarbene complexes.^{13,14}

If the above method is performed in a stepwise procedure of lithiations and reactions with the appropriate metal carbonyls, the method allows for the preparation of mixed metal biscarbene complexes.¹⁴ To illustrate this, the mixed dimetal biscarbene complex **5** [Cr(CO)₅C(OEt){C₆H₂S₂}C(OEt)W(CO)₅] was prepared. The addition of a single equivalent of both thieno[2,3-*b*]thiophene and *n*-BuLi was followed by the addition of one equivalent of chromium hexacarbonyl to form the chromium acylate. The reaction was continued by the addition of a second equivalent of *n*-BuLi followed by an equivalent of tungsten hexacarbonyl, forming the heterobimetallic bisacylate. The reaction was completed by alkylating with excess triethyloxonium tetrafluoroborate. After gradient elution on a silica gel column, four products, **1**, **2**, **3** and **5** (Scheme 2), were isolated. The outcome of the reaction was only moderately successful with the desired mixed dimetal biscarbene complex representing only a quarter of the products in the reaction mixture. The simultaneous formation of some dilithiated species during the first lithiation step and reaction with a metal carbonyl resulted in homogenous metal carbene formation. The main product, after the first lithiation and reaction with the chromium hexacarbonyl, was the monochromium acylate along with a significant portion of the 5,5'-bisacyldichromate. In addition, the monocarbene of tungsten carbonyl also formed and indicated that a portion of the thieno[2,3-*b*]thiophene was not lithiated during the initial reaction with *n*-BuLi. The absence of ditungsten biscarbene complex **4** confirmed that an excess of *n*-BuLi was not used during the second lithiation. Nevertheless, the stepwise acylate-formation method was successful in producing a workable yield of the heterobimetallic Fischer biscarbene complex **5**. Compounds **1** and **2** were purified by column chromatography and crystallization, while **3** and **5** were collected as one fraction and co-crystallize from a dichloromethane–hexane mixture.



Scheme 2: Synthesis of a mixed metal biscarbene complex of thieno[2,3-*b*]thiophene. (i) 1 eq. *n*-BuLi, (ii) 1 eq. M(CO)₆ or M'(CO)₆, (iii) excess [Et₃O][BF₄].

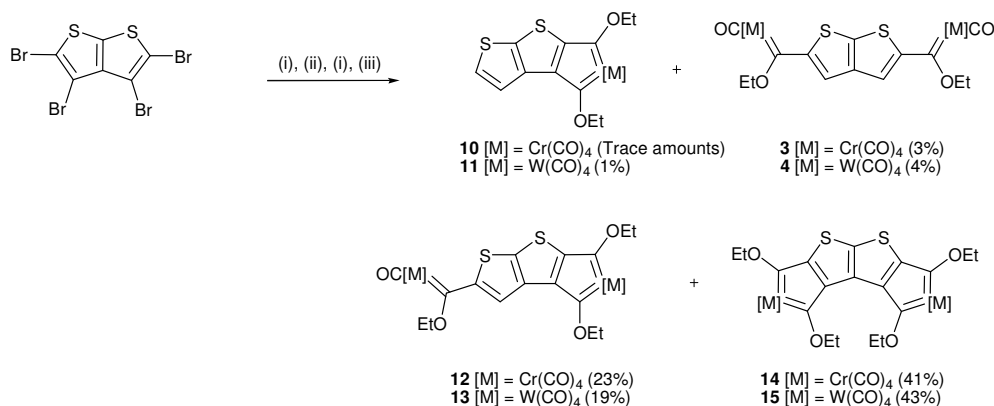
The scope of Fischer carbene synthesis is highlighted when the characteristics of lithium–hydrogen (deprotonation) and lithium–halogen exchange reactions are carefully combined and exploited to selectively target lithiations at specific sites on the thiophene substrates. The formation and chelation of biscarbene ligands require the second lithiation to occur at an adjacent, normally less reactive, site on the thiophene ring. Hence, activating the less reactive β -positions by a favoured lithium–halogen exchange reaction is feasible. The trick for preparing such chelated carbene complexes on a thiophene ring is not to prepare the unstable 1,2-dianion, but to sequentially produce an anion which forms the first metal acylate and can immediately stabilize the formation of the second anion. The synthesis of **6** and **7** is optimized by reacting 3-bromothiophene with one equivalent lithium diisopropylamine (LDA). LDA favours deprotonation at the 2-position of thiophene and leaves the bromo–substituent unaffected in the 3–position. As a result, this will generate the key intermediate 3-bromo-2-lithiothiophene (**D**); the ideal precursor for generating two adjacent reaction positions. Reacting **D** with a metal hexacarbonyl results in the metal acylate with the negative charge delocalized over the metal carbonyl moiety. The acylate is subsequently converted into a 2,3-metallocyclic bisacylate intermediate through the addition of an equivalent of *n*-BuLi. Alkylation with excess $[\text{Et}_3\text{O}][\text{BF}_4]$ affords **6** and **7** in moderate yields (Scheme 3a). Intermediate **D** is also accessible using *n*-BuLi instead of LDA, but in lower yields. In this instance a lithium–bromine exchange reaction is favoured and gives 3-lithiothiophene which immediately participates in a *trans*-lithiation reaction with a second 3-bromothiophene, yielding **D**.



Scheme 3: Synthesis of thiophene chelates from 3-bromothiophene (a) and tetrabromothiophene (b): (i) 1 eq. LDA, (ii) 1 eq. $\text{M}(\text{CO})_6$, (iii) 1.2 eq. *n*-BuLi and (iv) excess $[\text{Et}_3\text{O}][\text{BF}_4]$.

The synthesis of the bischelated tetracarbene complexes **8** and **9** was targeted. The most stable position for anion formation is at the most acidic proton in the thiophene's α -position. Thus, it is not necessary to remove α -bromo-substituents of tetrabromothiophene to form 3,4-dibromothiophene in order to prepare the bischelated tetracarbene complexes of thiophene **8** and **9** directly from substrate tetrabromothiophene. The best method was to dilithiate with 2.5 equivalents *n*-BuLi at the α -positions and react the lithiated species with two equivalents of metal hexacarbonyl to give 2,5–dinuclear bisacylates (Scheme 3b). The acyl charge is delocalized over the metal pentacarbonyl fragments, facilitating the lithium–bromine exchange reaction in the 3- and 4-thiophene positions on addition of a second portion of 2.5 equivalents *n*-BuLi. Intramolecular reactions with a second carbonyl ligand on each of the metal pentacarbonyl units on either side of the thiophene ring resulted in the formation of two bisacylate chelate rings. Alkylation with excess $[\text{Et}_3\text{O}][\text{BF}_4]$ afforded the dichelated tetraethoxycarbene complexes (**8**, **9**). Similarly, the precursor 4,4'-dibromo-thieno[2,3-*b*]thiophene was considered a suitable substrate to extend the thiophene work to the fused thieno[2,3-*b*]thiophene system, as it would require the combination of deprotonation (5- and 5'-positions) and lithium–halogen exchange reactions

(4- and 4'-positions). However, the synthesis of 4,4'-dibromothieno[2,3-*b*]thiophene requires the initial formation of 4,4',5,5'-tetrabromothieno[2,3-*b*]thiophene, followed by the debromination of the 5- and 5'-positions.^{11,15} Thus, as the thiophene results indicated that it was possible to obtain both mono- and bischelated carbene complexes from the tetrabromothiophene precursor, 4,4',5,5'-tetrabromothieno[2,3-*b*]thiophene was chosen as substrate to target the formation of both classes of chelated complexes (**10**, **11**, **14** and **15**). The reaction of 4,4',5,5'-tetrabromothieno[2,3-*b*]thiophene with 2.4 equivalents of *n*-BuLi, 2 equivalents of metal carbonyl and another addition of 2.4 equivalents *n*-BuLi, afforded a number of carbene complexes. In Scheme 4 the products isolated and their yields are indicated. They are $[M(CO)_5\{C(OEt)C_6H_2S_2C(OEt)\}M(CO)_5]$ ($M = Cr$ **3**, **4**), $[M(CO)_4\{C(OEt)\}_2C_6H_1S_2C(OEt)M(CO)_5]$ ($M = Cr$ **12**, **13**) and $[M(CO)_4\{C(OEt)\}_2C_6S_2\{C(OEt)\}_2M(CO)_4]$ ($M = Cr$ **14**; **15**) and trace amounts of $[M(CO)_4\{C(OEt)\}_2C_6H_2S_2]$, ($M = Cr$ **10**, **11**).



Scheme 4: Synthesis of chelated biscarbene complexes: (i) 2.4 eq. *n*-BuLi, (ii) 2 eq. Cr(CO)₆ or W(CO)₆, (iii) excess [Et₃O][BF₄].

The first lithiation occurs at an α -position and the second at the other α -position. If no further lithium reagent was used after reaction with the metal carbonyl and alkylation, the resulting reaction products were the dinuclear biscarbene complex of the particular metal used (**3**, **4**). The formation of biscarbene complexes **3**, **4**, **10** and **11**, in very low yields, provides evidence of incomplete lithiations. The addition of a further 2.4 equivalents of *n*-BuLi yielded the desired bischelated tetra-acylates, which result in the bischelated neutral tetracarbene complexes **14** and **15** after alkylation. Incomplete lithiation during the second lithiation step results in the precursor intermediates for the unique complexes **12** and **13**. These complexes never formed in the corresponding reaction with tetrabromothiophene. The greater stability of thieno[2,3-*b*]thiophene tris-acylate intermediates is ascribed to a lack of inter-ring delocalization, similar to isolated monocarbene complexes. Alkylation of the reaction mixture with a large excess [Et₃O][BF₄] affords the desired bischelated tetracarbene complexes **14** and **15** as well as **12** and **13**, in significant yields. The Fischer carbene complexes **12** and **13** are without precedent in literature and represent the combination of two different classes of carbene ligands (monocarbene and chelated biscarbene on opposite sides of the thieno[2,3-*b*]thiophene). A large excess of alkylating agent has been implicated experimentally to play a role in the removal of remaining bromines from intermediates.¹⁶ The formation of **10** and **11**, in low yields, indicates a lithium-halogen exchange reaction at a less favoured reaction site (4-position) while a more reactive site (5'-position) was still available and remained unaffected. The chelated biscarbene complexes are relatively stable, although flash chromatographic methods were employed for separation.

Spectroscopic Characterization

In the ^1H NMR spectra of **1–5**, **12** and **13**, the H4 chemical shift of thieno[2,3-*b*]thiophene is most affected by the adjacent substitution of H5 with an electron-withdrawing carbene carbon. A significant downfield shift is observed, compared to the α - and β -proton chemical shifts of thieno[2,3-*b*]thiophene at 7.38 and 7.27 ppm, respectively (remeasured in CDCl_3).¹⁷ The proton chemical shifts of the thiophene ring furthest from the carbene carbon in **1** and **2** are little affected compared to those of the thieno[2,3-*b*]thiophene substrate, indicating little inter-ring delocalization. In the monochelated biscarbene complex **10** and **11** only a small downfield shift is observed for both remaining ring protons (Cr: 7.45 and 7.39 ppm and W: 7.49 and 7.45 ppm). The corresponding chemical shifts of the α -protons are further downfield (Cr 7.56 and W 7.60 ppm) and the β -protons slightly upfield (Cr 6.84 and W 6.92 ppm) in **6** and **7** compared to the corresponding shifts of thiophene at 7.20 and 6.96 ppm, respectively.¹⁸ The H4 chemical shifts of the biscarbene complexes **3** and **4** are slightly more downfield, because of the effect of two *versus* one electron-withdrawing Fischer carbene carbon, compared to that for **1** and **2**. The furthest downfield thieno[2,3-*b*]thiophene chemical shifts of H4 are found for **12** (8.61 ppm) and **13** (8.59 ppm, Figure 2). Interestingly the chemical shifts of the protons in the 4- and 5-positions of both thiophene and thieno[2,3-*b*]thiophene are little affected by the presence of a fused metallocyclic biscarbene chelate ring on the opposite side of the thiophene ring(s) in **6**, **7**, **10** and **11**. The downfield shifts of the methylene protons of the ethoxycarbene substituents are very sensitive to changes in the electronic properties of the carbene carbon atom. The metal-sensitive methylene resonances of Cr complexes are shifted downfield by *ca* 0.2 ppm compared to their W analogues. The ^1H NMR spectrum of **5** represents a combination of the spectra of **3** and **4** with almost identical chemical shifts and emphasizes the individuality of each thiophene ring in **5**.

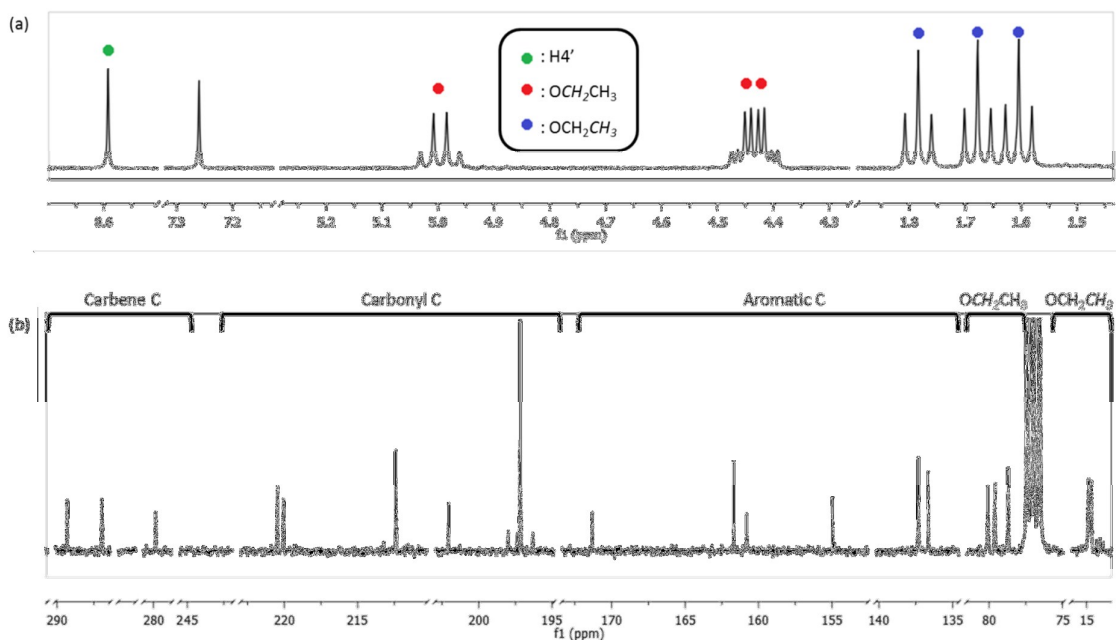


Figure 2: The ^1H NMR (a) and ^{13}C NMR (b) spectra (CDCl_3) of **13** displaying the chemical shifts of the three electronically different carbene ligands.

The ^1H NMR spectrum of the triscarbene complex **13**, shown in Figure 2a, displays the characteristic features of mono-, bis- and chelated multicarbene complex-types representative of all complexes in this study. All three carbene ligands are unique and resonate in different chemical environments. The same patterns and trends of chemical shifts of the protons, for the different metals, are observed for the chelated biscarbene analogues (**6–15**). The methylene protons of the mono- and biscarbene complexes with thienyl substituents resonate around 5.2–5.0 ppm, while the same chemical shifts in the chelated carbene complexes are shifted significantly upfield (around 4.5–4.8 ppm). The latter now falls within the region normally associated with methylene resonances of ester groups. The shifts indicate a smaller involvement of the ethoxy group in stabilizing the carbene carbon, highlighting the role of both the annulated thiophene ring and the attached metalocycles in stabilizing the biscarbene ligands of the chelate ring. Based on resonance structures (Figure 3) and observations reported for chelated biscarbene complexes of thiophene, assignments were made with the more downfield chemical shift belonging to the ethoxy substituent of the carbene with its carbon furthest from the sulfur atom in the thiophene ring.

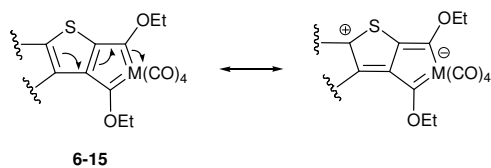


Figure 3: Electron delocalization from the adjacent thiophene ring, through π -resonance effects, affecting the carbene ligands in the chelate ring.

Table 1: Selected downfield ^{13}C NMR chemical shifts (ppm, in solvent CDCl_3) of the complexes **1–15**.^a

Complex	$\text{M}(\text{CO})_5$		$\text{M}(\text{CO})_4$		C_{ipso}	
	$\text{C}_{\text{carb}}^{\text{b}}$	CO_{trans}	CO_{cis}	CO_{trans}		CO_{cis}
1	313.6	223.1	217.1		157.7	
2	288.3	202.3	197.6		160.6	
3	315.3	223.0	216.8		158.2	
4	289.5	202.2	197.3		161.7	
5 (Cr)	315.5	223.1	216.8		158.3	
(W)	289.3	202.2	197.3		161.5	
6	320.9, 312.2			242.5, 241.7	227.1	167.2, 163.2
7^c	313.9, 283.3			n.o., 201.1	191.1	164.7, n.o.
8	316.5, 301.7			245.5, 239.5	226.0	165.0, 151.6
9^c	317.8, 283.7			212.4, 209.1	194.8	165.4, 158.3
11	289.3, 281.8			220.4, 220.2	212.4	171.4, 160.2
12	314.9, 307.2			243.8, 243.5	228.1	158.6, 156.9
	315.1	223.0	216.7			164.4
13	286.9, 279.8			220.5, 220.1	212.4	161.7, 160.8
	289.3	202.1	197.2			171.3
14	319.5, 310.7			242.3, 239.4	227.0	164.1, 159.8
15	293.8, 283.7			219.5, 217.2	211.6	170.0, 163.5

^a ^{13}C NMR spectrum of **10** not recorded. ^b carb = carbene. ^c Measured in C_6D_6

The ^{13}C NMR chemical shifts of the carbene and carbonyl carbons as well as the carbon *ipso* to the carbene carbon are summarized in Table 1. Measurements in C_6D_6 give chemical shifts upfield compared to those measured in CDCl_3 . Figure 2b shows the ^{13}C NMR spectrum of **13** which is representative of chemical shifts found for the mono-, bis- and chelated biscarbene complexes and divides the spectrum into different chemical shift regions. The chemical shifts of the carbene carbons are metal sensitive with the chromium monocarbene carbons (301–319 ppm) further downfield than the corresponding tungsten complexes (280–294 ppm). The carbonyl carbon chemical shifts for $\text{M}(\text{CO})_5$ are around 223 (*trans*) and 217 ppm (*cis*) for chromium while the tungsten shifts are around 202 (*trans*) and 197 ppm (*cis*). The metal tetracarbonyl fragments display three peaks in the ^{13}C NMR spectra and the chemical shifts are found more downfield than those of the pentacarbonyl moieties. The two smaller peaks furthest downfield in the carbonyl region represent the carbonyl ligands *trans* to the two carbene carbons, indicating that they resonate in different electronic environments. The larger peak less downfield represents the two *cis* carbonyl ligands, which are *trans* to each other. The chemical shift values for the metal carbonyl moieties are characteristic of a specific metal and the difference in chemical shift values of the carbonyl resonances is approximately 20 ppm for the chromium and tungsten complexes. The resonances of the *ipso*-carbons attached to carbene carbons are very similar, with the tungsten carbene complexes being shifted slightly further downfield compared to the corresponding chromium carbene complexes.

The number, pattern and positions of the infrared bands in the carbonyl region of the infrared spectra confirm the presence of $\text{M}(\text{CO})_5$ fragments in **1–5** and **12**, **13** and *cis*- $\text{M}(\text{CO})_4$ fragments in **6–15**.¹⁹ Characteristic of the biscarbene complexes (**3**, **4** and **5**) is the duplication of the $\text{A}_1^{(1)}$ band (Figure 4), the reason speculatively ascribed to the existence of two different orientated vibrational modes for the two equatorial planes of *cis*-carbonyl ligands in the complexes. The IR spectrum of the tungsten complex **4** displayed higher wavenumbers for the $\text{A}_1^{(1)}$ band compared to the chromium analogue **3**, but this order is reversed for the vibrational frequencies at lower wavenumbers ($\text{A}_1^{(2)}$ and E modes). The vibrational frequencies of **5** fall between the values of **3** and **4**. Complexes **12** and **13** contain both *cis*-tetra- and pentacarbonyl fragments. The $\text{A}_1^{(2)}$ and E carbonyl stretching vibrational modes of the $\text{M}(\text{CO})_5$ fragment overlap with the B_1 mode of the *cis*- $\text{M}(\text{CO})_4$ fragment of **13**, resulting in poor resolution that complicates assignments.

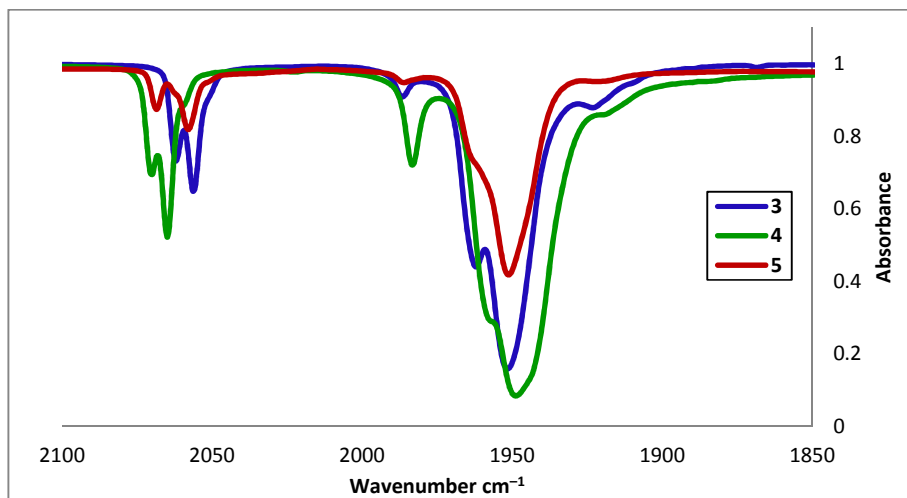


Figure 4: Comparison of the ν_{CO} bands displayed by **3**, **4** and **5**.

Structural studies of the carbene complexes.

The molecular structures of **2**, **4**, **5**, **7**, **13** and **15** (Figure 5–8) were studied by single crystal X-ray diffraction analyses. The crystal structures display a planar thiophene or thieno[2,3-*b*]thiophene moiety attached to a metal carbonyl fragment and an ethoxycarbene substituent. In **5**, the crystal structure refinement indicated 68% chromium and 32% tungsten at one metal location (Cr1/W1) and 70% chromium and 30% tungsten at the other metal location (Cr2/W2). This means that **3** co-crystallized with **5** in a ratio of 38:62 and was confirmed by peak integration in the ^1H NMR spectrum of **5**. The mono- and biscarbene complexes (**1**–**5**) all have the ethoxy substituent on the same side of the adjacent thiophene sulfur atom, while the orientation of the ethoxy substituents in **6**–**15** are determined by the rigidity of the chelate rings.

In the molecular structures, one linear pair of the *cis*-pentacarbonyl ligands usually bend away from the carbene. By contrast, the pair of *cis*-tetracarbonyl ligands, perpendicular to the chelate ring, bend towards the chelate ring. For the mono- and biscarbene complexes (**2**, **4** and **5**) as well as **13**, only one pair of the *cis*-pentacarbonyl ligands, per complex, were shown to bend away significantly. For **2** this deviation from linear is $-9.2(1)^\circ$, while the greatest deviations in **4** and **5** are $\approx -7^\circ$. In the tetracarbonyl complexes the greatest deviations of the *cis*-carbonyl ligands are in **15** ($7.7(1)^\circ$ and $5.6(1)^\circ$ respectively).

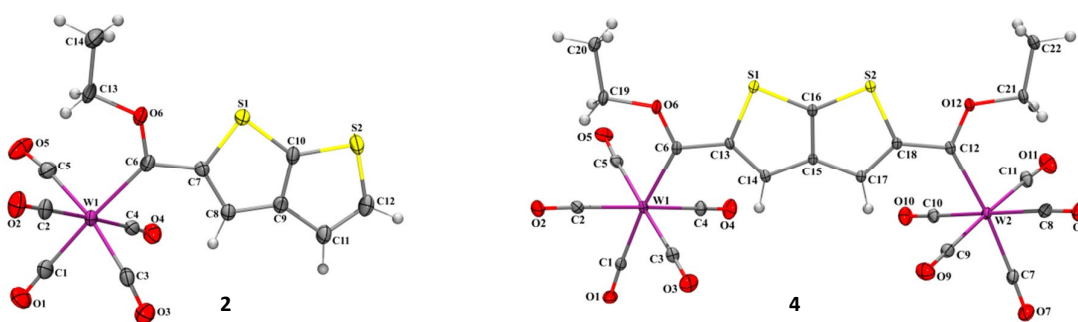


Figure 5: Molecular structure representation of **2** and **4** (thermal ellipsoids are shown with 50% probability).

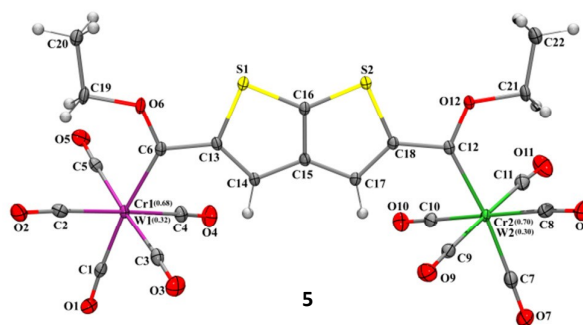


Figure 6: Molecular structure representations of **5** (thermal ellipsoids are shown with 50% probability).

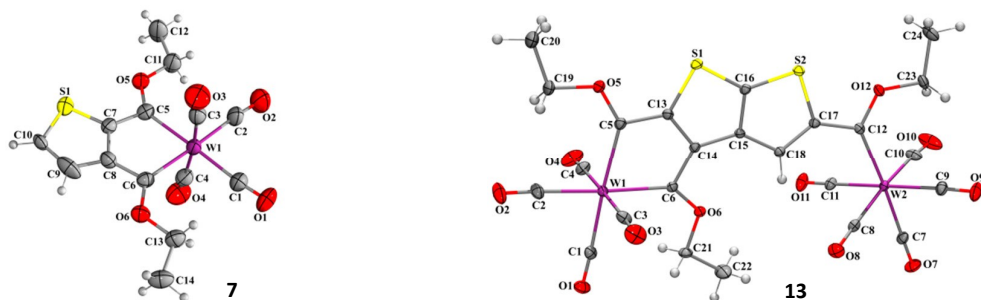


Figure 7: Molecular structures of **7** and **13** (thermal ellipsoids are shown with 50% probability). The DCM molecule, per two molecules of **13**, is not shown for simplicity.

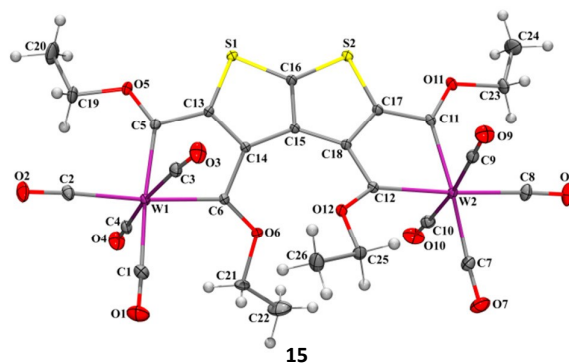


Figure 8: Molecular structure representation of **15** (thermal ellipsoids are shown with 50% probability).

The inter-ring torsion angles of thieno[2,3-*b*]thiophene confirm that the planarity of the thieno[2,3-*b*]thiophene linker is retained in the structures, irrespective of the number of metal moieties in the carbene complexes. All structures display only small deviations from planarity for the condensed thieno[2,3-*b*]thiophene ring with the carbene carbons and the torsion angles ($C_{\text{carb}}-C_{\text{ipso}}-C_{\beta}-C9/15$ and $C_{\text{carb}}-C_{\text{ipso}}-C9/15-C10/16$) deviate with less than 7° , with the exception of **15**. With only one ethoxy substituent in **13**, on the opposite side of the sulfur atoms, the steric repulsion in this part of the molecule is far less compared to that in **15**. As a result, the three-ring linker in **13** deviates less from planarity compared to the four rings in **15**. This deviation from the backbone is the result of steric constraints caused by the metal tetracarbonyl and ethoxy fragments. The torsion angles also indicate that the ethoxy groups of **15** (especially on the opposite side of the sulfur atoms) are bent out of the mean plane, in order to alleviate the steric congestion and retain ring planarity as far as possible (Figure 9). The distortion in this part of the molecule is illustrated by the short non-bonding distance between O6 and O12 (2.693 Å) and the torsion angle O12...C18...C14...O6 (-45.65°). This effect of the close proximity of the two non-bonded oxygen atoms in **15**, forces the C6 and C12 carbene carbons out of the ring plane ($17.3(2)^\circ$ and $16.6(2)^\circ$, below and above respectively).

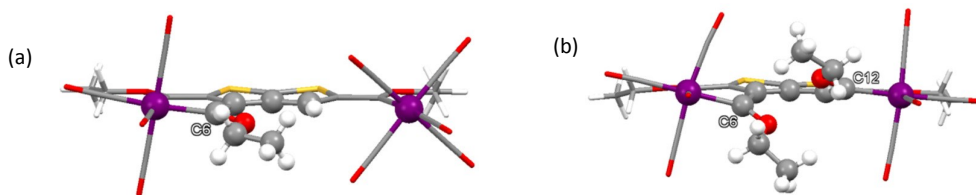


Figure 9: Orientation of the planar bridging thienothiophene moiety and ethoxycarbene substituents of **13** (a) and **15** (b), viewed parallel with the mean plane through thieno[2,3-*b*]thiophene.

The W—C_{carb} bond length in **2** (2.214(3) Å) is slightly longer than those in **4** (averaged 2.197(3) Å) and the analogous thiophene biscarbene complex (averaged 2.191(5) Å).^{5b} The significantly shorter W—C_{carb} bond distances of the chelate rings are ascribed to restrictions imposed by the ring size and electronic effects resulting from chelation. The role of ring strain is further emphasized by a small decrease in the W—C_{carb} bond distances on going from **13** to **15** as well as a shorter C—S distance (S2—C_{out}) in the thienothiophene unit when adjacent to a chelate biscarbene ring. The chelate rings affect the geometry around the carbene carbons of **13** and **15**. This manifests in a smaller W—C_{carb}—C angle compared to the corresponding angles in **2**, **4** and **5**, and a noticeable increase in the angle between the tungsten pentacarbonyl and the ethoxy moiety of the chelated carbene carbons. For the thieno[2,3-*b*]thiophene linker, the C—C bond lengths show consecutive shorter–longer bond distances, retaining single and double bond character of the uncoordinated thieno[2,3-*b*]thiophene fragment. For comparison, the C—C bond distances in 4,4-dibromothieno[2,3-*b*]thiophene are 1.358(8), 1.429(7) and 1.374(7) (internal).¹¹ The C—C bond common to both the chelate and the thiophene rings, have similar distances for **7**, **13** and **15**.

Table 2: Selected bond lengths, bond angles and torsion angles for **2**, **4**, **5**, **7**, **13** and **15**.

Complex/atoms	2	4	5	7	13	15
Bond lengths (Å)						
W1—C5				2.164(3)	2.170(2)	2.149(2)
W/Cr1—C6	2.214(3)	2.196(2)	2.121(2)	2.175(3)	2.168(2)	2.156(2)
W2—C11/C12					2.184(2)	2.162(2)
W/Cr2—C12		2.197(3)	2.120(3)			2.160(2)
C5—O5				1.317(3)	1.316(2)	1.322(2)
C6—O6	1.328(4)	1.326(3)	1.325(3)	1.305(4)	1.316(2)	1.309(2)
C12/C11—O12/C11		1.318(3)	1.319(3)		1.324(2)	1.321(2)
C12—O12						1.316(2)
C5/C6—C7/C13	1.46(1)	1.460(3)	1.462(3)	1.450(5)	1.446(3)	1.458(3)
C6—C14/C8				1.452(5)	1.462(3)	1.472(2)
C12/C11—C18/C17		1.460(3)	1.466(3)		1.463(3)	1.449(3)
C12—C18						1.470(3)
W—C(CO) _{trans}	2.016(3)	2.017(3)	1.912(3)	2.013(4) ^a	2.011(2) ^a	2.026(2) ^a
		2.026(3)	1.917(3)		2.028(2)	2.019(2) ^a
W—C(O) _{cis} ^a	2.037(3)	2.040(3)	1.947(3)	2.062(6)	2.053(2)	2.057(2)
		2.040(3)	1.942(3)		2.043(2)	2.055(2)
S1—C _{outside}	1.769(9)	1.765(2)	1.770(3)	1.703(4)	1.739(2)	1.733(2)
S2—C _{outside}	1.738(9)	1.763(3)	1.769(3)	1.74(1)	1.768(2)	1.738(2)
S1—C _{inside}	1.712(6)	1.709(3)	1.708(3)		1.717(2)	1.719(2)
S2—C _{inside}	1.718(6)	1.707(2)	1.710(2)		1.706(2)	1.724(2)
C=C _{outside}	1.38(1)	1.367(4)	1.367(4)	1.385(5)	1.383(3)	1.378(2)
	1.38(1)	1.378(3)	1.365(3)	1.39(2)	1.377(3)	1.384(3)
C=C _{inside}	1.39(1)	1.389(3)	1.384(4)		1.395(3)	1.398(3)
C—C	1.419(8)	1.415(3)	1.415(3)	1.396(9)	1.427(3)	1.429(2)
	1.437(8)	1.413(3)	1.418(3)		1.413(3)	1.427(3)

Bond Angles (°)						
W1—C _{carb} —O	128.6(2)	129.9(2)	130.1(2)	136.8(3)	137.4(2)	138.3(2)
				136.5(3)	137.1(1)	136.6(1)
W2—C _{carb} —O		129.7(2)	129.9(2)		130.0(1)	137.8(2)
						136.3(1)
W1—C _{carb} —C	125.5(4)	124.0(2)	124.4(2)	113.3(2)	112.9(1)	112.3(1)
				112.8(2)	114.3(1)	113.6(1)
W2—C _{carb} —C		123.5(2)	123.5(2)		124.5(1)	113.0(1)
						114.8(1)
O—C _{carb} —C(W1)	105.6(5)	106.0(2)	105.4(2)	109.9(3)	109.7(2)	109.4(2)
				110.7(3)	108.5(2)	109.6(2)
O—C _{carb} —C(W2)		106.8(2)	106.5(2)		105.5(2)	109.2(2)
						108.5(2)
C _{carb} —W1—C _{carb}				78.2(1)	77.6(1)	76.6(1)
C _{carb} —W2—C _{carb}						77.4(1)
Torsion Angles (°)						
C _{carb} —C _{ipso} —C _β —C9/15	-173.2(8)	179.9(2)	-179.7(2)	179.0(6)	-177.8(2)	177.9(2)
		-177.0(2)	-177.5(2)	-178(1)	-178.4(2)	-179.0(2)
C _{carb} —C _{ipso} —C9/15—C10/16					177.4(2)	162.7(2)
						163.4(2)

^aAveraged, ^bC2 and C3 indicate the shared internal carbons between the two thiophene rings in thieno[2,3-*b*]thiophene

Crystal packing properties of 5, 7, 13 and 15. The packing of **5**, **7**, **13** and **15** varies from grid-like networks (Figure 10a and b (**5** and **7**)), to “wheels” (Figure 10c (**13**)) to parallel corrugated lines (Figure 10d (**15**)), maintained at least in part by intermolecular hydrogen interactions. These intermolecular hydrogen interactions (O⋯H) occur predominantly between the oxygen of the carbonyl ligand and a hydrogen on the methylene or methyl group. The hydrogen interactions range from 2.430 to 2.712 Å. No π-stacking interaction of the (thieno)thiophene rings was observed, with the shortest distance between any of the rings being larger than 4 Å. Compounds **4** and **5** pack in a similar fashion, with the same intermolecular interactions. The complexes undergo columnar packing when viewed down two different axes respectively, with the molecules fitting on top of each other down the column. This basic structural motif (columns) can be divided into different levels of crystal organization, primary (columns) and secondary (layers of columns).²⁰ The packing of **5**, viewed down the crystallographic *a*-axis, shows columns that are parallel-packed together in an interlocked non-planar fashion. The thiophene rings stack in the crystal structure but without π-π interaction (separation distance of 13.056 Å). The formation of a grid-like network is evident from the view along the crystallographic *a*-axis, Figure 10a, consisting of two dimers that pack antiparallel to each other. In the case of **7**, the grid-like network consists of two dimers that pack parallel to each other and the O⋯H interactions now occur predominantly between the oxygens of carbonyl ligands and the α-hydrogen of a thiophene ring or a hydrogen on the methylene or methyl group. (Figure 10b). The packing of **13**, viewed down the crystallographic *c*-axis, consists of columns of “wheels” that pack parallel to each other. Each “wheel” contains two dimers that pack antiparallel to each other, with the four chelated rings facing to the outside, Figure 10c. Corrugated lines consisting of antiparallel-packed dimers, in the vertical direction, is observed for **15** when viewed down the crystallographic *c*-axis, Figure 10d.

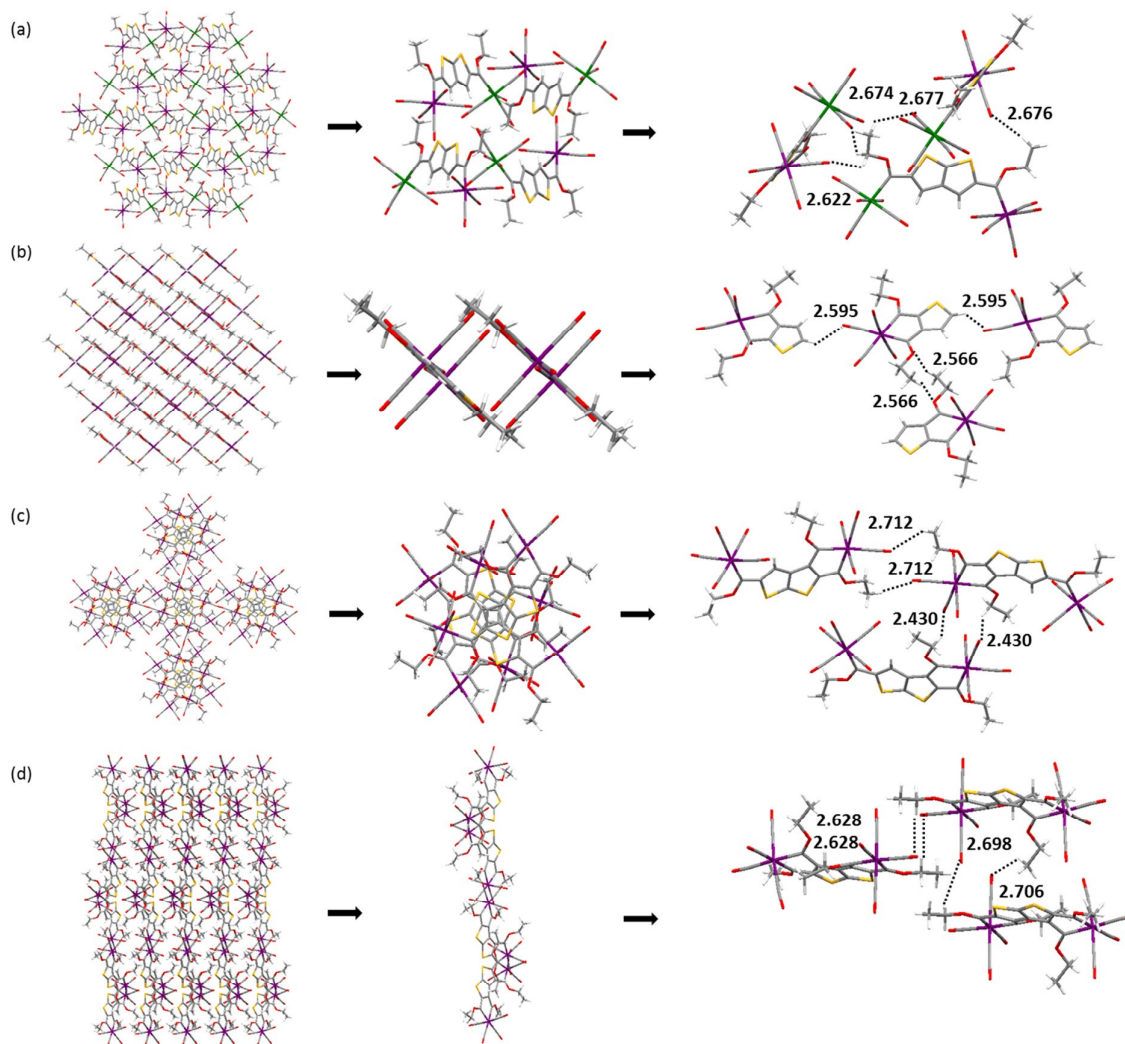


Figure 10: Packing features of **5** (a) when viewed down the crystallographic a -axis, **7** (b) viewed down the crystallographic b -axis, **13** (c) and **15** (d) viewed down the crystallographic c -axis.

Experimental Section

General. Thiophene, tetrabromothiophene, thieno[2,3-*b*]thiophene, 1,4-bis(trimethylsilyl)-1,3-butadiyne, *n*-BuLi (1.6 M solution in hexane), chromium and tungsten hexacarbonyls were purchased from Sigma Aldrich and Strem Chemicals and used as received. Thieno[2,3-*b*]thiophene can be prepared from trimethylsilyl-1,3-pentadiyne,¹¹ while procedures from literature were employed for the preparation of 4,4',5,5'-tetrabromothiopheno[2,3-*b*]thiophene²¹ and triethyloxonium tetrafluoroborate.²² All operations were carried out using standard Schlenk techniques under an inert atmosphere of nitrogen or argon. Silica gel 60 (particle size 0.063–0.20 mm) was used as resin for all column chromatography separations. Anhydrous THF (tetrahydrofuran) and hexane were distilled over sodium metal and DCM (dichloromethane) over CaH₂. NMR spectra were recorded on Bruker ADVANCE 500, Ultrashield Plus 400 AVANCE 3 and Ultrashield 300 AVANCE 3 spectrometers, at 25°C, using CDCl₃ and/or C₆D₆ as solvent. The ¹H NMR spectra were recorded at 500.139, 400.13 or 300.13 MHz, and the ¹³C NMR spectra at 125.75, 100.613 or 75.468 MHz. The chemical shifts were referenced to deuterated chloroform (CDCl₃) signals at 7.26 ppm for δH and 77.00 ppm for δC, or deuterated benzene at 7.16 ppm and 128.00 ppm, respectively. Numerical numbering of atoms for NMR spectral assignments is indicated in Figure 11. Infrared spectroscopy was performed on a Bruker ALPHA FT-IR spectrophotometer with a NaCl cell, using hexane as solvent. Mass spectral analyses were performed on a Synapt G2 HDMS, by direct infusion at 10 μL/min, with negative electron spray as ionization technique for compounds **1–5** and **10–15**. Samples were made up in 100% MeOH to an approximate concentration of 10 μg/mL. The *m/z* values were measured in the range of 100–1500. Elemental analysis data for **6–9** were obtained from a ThermoScientific Flash 2000 organic elemental analyser.

Crystallography. Single crystal diffraction data for **2**, **4**, **5**, **13** and **15** were collected at 150 K on a Bruker D8 Venture diffractometer with a kappa geometry goniometer and a Photon 100 CMOS detector using a Mo-Kα 1μS.micro focus source. Data for **7** were collected at 293 K on a Siemens P4 diffractometer fitted with a Bruker SMART 1 K CCD detector using graphite-monochromated Mo-Kα radiation by means of a combination of phi and omega scans. Data were reduced and scaled using SAINT.²³ Absorption corrections were performed using SADABS.²³ The structures were solved by a novel dual-space algorithm using SHELXTS²⁴ (**2**, **4**, **5**, **13** and **15**) or by direct methods (**7**) and were refined by full-matrix least-squares methods based on *F*² using SHELXL.²⁵ All non-hydrogen atoms were refined anisotropically. All hydrogen atoms were placed in idealized positions and refined using riding models. The CIF files for complexes **2**, **4**, **5**, **7**, **13** and **15** are available as Supporting Information.

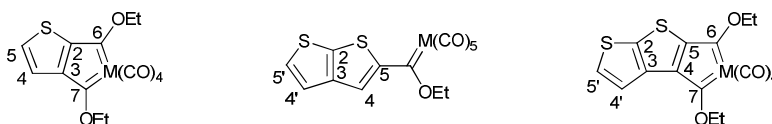


Figure 11: Numerical proton and carbon assignments used for thiophene, thieno[2,3-*b*]thiophene and carbene substituents.

Preparation of thieno[2,3-*b*]thiophene carbene complexes: [Cr(CO)₅C(OEt){C₆H₃S₂}] (**1**), [W(CO)₅C(OEt){C₆H₃S₂}] (**2**), [Cr(CO)₅C(OEt){C₆H₂S₂}C(OEt)Cr(CO)₅] (**3**), [W(CO)₅C(OEt){C₆H₂S₂}C(OEt)W(CO)₅] (**4**). A solution of 0.19 mL (1.8 mmol) of thieno[2,3-*b*]thiophene in 15.0 mL of THF was treated with 1.64 mL (2.6 mmol) of *n*-BuLi at –78°C. After stirring for 30 min., Cr(CO)₆ (0.58 g, 2.6 mmol) or W(CO)₆ (0.93 g, 2.6 mmol) was added to the solution and stirred for a further 15 min in the cold and then allowed to reach room temperature over 40 min. The solvent was removed under reduced pressure and the residue dissolved in 10 mL of DCM and cooled to –20°C. The reaction mixture was treated with 0.80 g (4.0 mmol) of

[Et₃O][BF₄] in DCM and subsequently allowed to reach room temperature. The reaction mixture was filtered through a small silica gel plug using DCM and the solvent was removed under reduced pressure. After absorbing the reaction mixture on silica, it was dry loaded onto a silica gel column. The respective products (**1–4**) were separated by column chromatography using gradient elution with hexane and DCM.

1: Yield: 0.33 g (0.8 mmol, 48 %), red crystals. ¹H NMR (CDCl₃, 300.13 MHz) δ: 8.41 (s, 1H, H4), 7.37 (s, 1H, H5'), 7.37 (s, 1H, H4'), 5.18 (q, 7.0 Hz, 2H, CH₂), 1.68 (t, 7.0 Hz, 3H, CH₃). ¹³C NMR (CDCl₃, 75.468 MHz) δ: 313.6 (C_{carb}), 223.1 ((Cr(CO)₅)_{trans}), 217.1 ((Cr(CO)₅)_{cis}), 157.7 (C5), 134.8 (C4), 147.4 (C3), n.o. (C2), 129.5 (C5'), 121.6 (C4'), 75.9 (CH₂), 15.1 (CH₃). IR (cm⁻¹, hexane, ν_{CO}): M(CO)₅: A₁⁽¹⁾ 2058 (m), B₁ 1983 (vw), A₁⁽²⁾ 1957 (sh), E 1947 (vs). Calc. C₁₄H₈O₆S₂Cr (387.92 g/mol) MS (m/z, intensity (%)); 274.89 (11%) [M-4CO-H]⁻.

2: Yield: 0.49 g, (0.9 mmol, 54%), red crystals. ¹H NMR (CDCl₃, 300.13 MHz) δ: 8.34 (s, 1H, H4), 7.39 (d, 5.3 Hz, 1H, H5'), 7.36 (d, 5.3 Hz, 1H, H4'), 5.00 (q, 7.1 Hz, 2H, CH₂), 1.66 (t, 7.1 Hz, 3H, CH₃). ¹³C NMR (CDCl₃, 75.468 MHz) δ: 288.3 (C_{carb}), 202.3 ((W(CO)₅)_{trans}), 197.6 ((W(CO)₅)_{cis}), 160.6 (C5), 135.7 (C4), 147.3 (C3), 148.2 (C2), 129.8 (C5'), 121.6 (C4'), 78.4 (CH₂), 14.9 (CH₃). IR (cm⁻¹, hexane, ν_{CO}): M(CO)₅: A₁⁽¹⁾ 2066 (m), B₁ 1979 (vw), A₁⁽²⁾ 1952 (sh), E 1943 (vs). Calc. C₁₄H₈O₆S₂W (519.93 g/mol) MS (m/z, intensity (%)); 564.87 (31%) [M+FA-H]⁻ (FA = formic acid).

3: Yield: 0.37 g (0.6 mmol, 33 %), purple crystals. ¹H NMR (CDCl₃, 300.13 MHz) δ: 8.47 (s, 2H, H4), 5.21 (q, 6.5 Hz, 4H, CH₂), 1.70 (t, 6.6 Hz, 6H, CH₃). ¹³C NMR (CDCl₃, 75.468 MHz) δ: 315.3 (C_{carb}), 223.0 ((Cr(CO)₅)_{trans}), 216.8 ((Cr(CO)₅)_{cis}), 158.2 (C5), 135.4 (C4), 147.2 (C3), 153.5 (C2), 76.3 (CH₂), 15.2 (CH₃). IR (cm⁻¹, hexane, ν_{CO}): M(CO)₅: A₁⁽¹⁾ 2062 and 2056 (m), B₁ 1986 (vw), A₁⁽²⁾ 1962 (sh), E 1952 (vs). Calc. C₂₂H₁₂O₁₂S₂Cr₂ (635.86 g/mol) MS (m/z, intensity (%)); 606.87 (28%) [M-CO-H]⁻.

4: Yield: 0.55 g (0.6 mmol, 35%), purple crystals. ¹H NMR (CDCl₃, 300.13 MHz) δ: 8.39 (s, 2H, H4), 5.01 (q, 7.1 Hz, 4H, CH₂), 1.68 (t, 7.1 Hz, 6H, CH₃). ¹³C NMR (CDCl₃, 75.468 MHz) δ: 289.5 (C_{carb}), 202.2 ((W(CO)₅)_{trans}), 197.3 ((W(CO)₅)_{cis}), 161.7 (C5), 135.8 (C4), 146.8 (C3), 154.9 (C2), 78.7 (CH₂), 14.9 (CH₃). IR (cm⁻¹, hexane, ν_{CO}): M(CO)₅: A₁⁽¹⁾ 2070 and 2065 (m), B₁ 1984 (vw), A₁⁽²⁾ 1955 (sh), E 1949 (vs). Calc. C₂₂H₁₂O₁₂S₂W₂ (899.88 g/mol) MS (m/z, intensity (%)); 898.88 (28%) [M-H]⁻.

Preparation of mixed metal biscarbene complex [Cr(CO)₅C(OEt){C₆H₂S₂}C(OEt)W(CO)₅] (5**).** A solution of 0.23 mL (2.2 mmol) of thieno[2,3-*b*]thiophene in 20.0 mL of THF was treated with 1.40 mL (2.2 mmol) of *n*-BuLi at -78 °C and stirred for 30 minutes. To the solution, Cr(CO)₆ (0.48 g, 2.2 mmol) was added and stirred for 15 min at cold temperature and then allowed to reach room temperature over 40 min. At -78 °C an additional portion of 1.40 mL (2.2 mmol) of *n*-BuLi was added and stirred for 30 minutes. The reaction was continued by the addition of W(CO)₆ (0.77 g, 2.2 mmol), stirred at -78 °C for 15 min, before allowing to reach room temperature over 40 min. The solvent was removed *in vacuo* and the residue dissolved in 10.0 mL of DCM and cooled to -20 °C. The reaction mixture was treated with 0.9 g (4.7 mmol) of [Et₃O][BF₄] in DCM and allowed to reach room temperature. The reaction mixture was filtered through a small silica gel plug using DCM and the solvent was removed under reduced pressure. The four products were purified by column chromatography using gradient elution with hexane and DCM. Yield: **1**: 0.23 g (0.6 mmol, 27%), **2**: 0.21 g (0.4 mmol, 18%), **3**: 0.24 g (0.7 mmol, 17%) and **5**: 0.35 g (0.5 mmol, 21%).

5: Yield: 0.35 g (0.5 mmol, 21%), purple crystals. ¹H NMR (CDCl₃, 400.13 MHz) δ: 8.47 (s, 1H, H4), 8.39 (s, 1H, H4'), 5.21 (q, 7.0 Hz, 2H, Cr(CH₂)), 5.01 (q, 7.1 Hz, 2H, W(CH₂)), 1.70 (t, 7.0 Hz, 3H, Cr(CH₃)), 1.68 (t, 7.2 Hz, 3H, W(CH₃)). ¹³C NMR (CDCl₃, 100.613 MHz) δ: 315.5 (C_{Cr-carb}), 289.3 (C_{W-carb}), 223.1 ((Cr(CO)₅)_{trans}), 216.8 ((Cr(CO)₅)_{cis}), 202.2 ((W(CO)₅)_{trans}), 197.3 ((W(CO)₅)_{cis}), 158.3 (C5), 135.3 (C4), 147.0 (C3), 154.2 (C2), 161.5 (C5'), 135.9 (C4'), 78.7 (W(CH₂)), 76.3 (Cr(CH₂)), 15.1

(Cr(CH₃)), 14.9 (W(CH₃)). IR (cm⁻¹, hexane, ν_{CO}): M(CO)₅: A₁⁽¹⁾ 2069 and 2058 (m), B₁ 1986 (vw), A₁⁽²⁾ 1963 (sh), E 1951 (vs). Calc. C₂₂H₁₂O₁₂S₂CrW (767.87 g/mol) MS (m/z, intensity (%)); 766.83 (6%) [M-H]⁻.

Preparation of the chelated biscarbene complexes: [Cr(CO)₄{C(OEt)}₂C₄H₂S] (6), [W(CO)₄{C(OEt)}₂C₄H₂S] (7) LDA was generated *in situ* from a mixture consisting of NⁱPr₂H (0.15 mL, 1.1 mmol) and *n*-BuLi (0.69 mL, 1.1 mmol) in THF and added dropwise to a solution of 3-bromothiophene (0.16 g, 1.0 mmol) in 15 mL THF at -90°C. The solution changed colour to light orange during stirring over a 20 min time period. Tungsten hexacarbonyl (0.35 g, 1.0 mmol) or chromium hexacarbonyl (0.22 g, 1.0 mmol) dissolved in 20 mL THF was added gradually to the reaction mixture. Stirring over a period of 1 h resulted in a colour change of the reaction mixture to red-brown. *n*-BuLi (0.69 mL, 1.1 mmol) in 10 mL THF was added to the reaction mixture at -78°C and stirring continued for an additional 1 h while the colour of the solution darkened. The solvent was removed *in vacuo* and the brown oily residue was dissolved in 30 mL cold (-30°C) DCM. The addition of [Et₃O][BF₄] (0.50 g, 2.5 mmol) dissolved in 10 mL DCM, resulted in the reaction mixture changing to an ink-blue colour. Completeness of alkylation was monitored by thin layer chromatography. Three products formed and were purified by column chromatography on silica using hexane as eluent. The first fraction (yellow) collected gave [M(CO)₅{C(OEt)Bu}] (less than 3%, W, Cr) and the second [M(CO)₅{C(OEt)C₄H₃S}] (15–17%, W, Cr),⁵ both known compounds. The third product was the major compound of the reaction and contains a chelating biscarbene ligand, [M(CO)₄{C(OEt)}₂C₄H₂S] M = Cr **6**, W **7**).⁵

6: Yield: 0.25 g (0.68 mmol, 68%), blue crystals. ¹H NMR (CDCl₃, 500.139 MHz) δ : 7.56 (d, 4.7 Hz, 1H, H5), 6.84 (d, 4.7 Hz, 1H, H4), 4.77 (q, 7.1 Hz, 2H, C3(CH₂)), 4.75 (q, 7.1 Hz, 2H, C3(CH₂)), 1.64 (t, 7.1 Hz, 3H, C3(CH₃)), 1.62 (t, 7.1 Hz, 3H, C2(CH₃)). ¹H NMR (C₆D₆, 400.13 MHz) δ : 6.60 (d, 4.8 Hz, 1H, H5), 6.43 (d, 5.1 Hz, 1H, H4), 4.48 (q, 7.1 Hz, 2H, C3(CH₂)), 4.46 (q, 7.1 Hz, 2H, C2(CH₂)), 1.12 (t, 7.1 Hz, 3H, C3(CH₃)), 1.09 (t, 7.1 Hz, 3H, C2(CH₃)). ¹³C NMR (CDCl₃, 125.75 MHz) δ : 320.9 (C3_{carb}), 312.2 (C2_{carb}), 242.5 ((Cr(CO)₄)_{trans}), 241.7 ((Cr(CO)₄)_{trans}), 227.1 ((Cr(CO)₄)_{cis}), 167.2 (C3), 163.2 (C2), 134.6, 116.7 (C5, C4), 76.8 (C3(CH₂)), 76.7 (C2(CH₂)), 15.2, 14.3 (CH₃). IR (cm⁻¹, hexane, ν_{CO}): Cr(CO)₄: A₁⁽¹⁾ 2020 (m), A₁⁽²⁾ 1964 (s), B₁ 1951 (s), B₂ 1902 (m). Anal. Calcd. (%) for C₁₄H₁₂O₆SCr (360.30 g/mol): C 46.67, H 3.36%. Found: C 46.84, H 3.45%.

7: Yield: 0.31 g (0.63 mmol, 63 %), blue crystals. ¹H NMR (C₆D₆, 500.139 MHz) δ : 6.96 (d, 5.3 Hz, 1H, H5), 7.31 (d, 5.1 Hz, 1H, H4), 4.45 (q, 7.1 Hz, 2H, C3(CH₂)), 4.44 (q, 7.1 Hz, 2H, C2(CH₂)), 1.68 (t, 7.1 Hz, 3H, C3(CH₃)), 1.65 (t, 7.1 Hz, 3H, C2(CH₃)). ¹³C NMR (C₆D₆, 125.75 MHz) δ : 313.9 (C3_{carb}), 283.3 (C2_{carb}), n.o. ((W(CO)₄)_{trans}), 201.1 ((W(CO)₄)_{trans}), 191.1 ((W(CO)₄)_{cis}), 164.7 (C3), n.o. (C2), 134.7, 117.7 (C5, C4), 78.6 (C3(CH₂)), 78.4 (C2(CH₂)), 14.9 (CH₃, overlapping). IR (cm⁻¹, hexane, ν_{CO}): M(CO)₄: A₁⁽¹⁾ 2028 (m), A₁⁽²⁾ 1956 (s), B₁ 1945 (s), B₂ 1892 (m). Anal. Calcd. (%) for C₁₄H₁₂O₆SW (492.15 g/mol): C 34.16, H 2.46%. Found: C 33.89, H 2.44%.

Preparation of the chelated biscarbene complexes: [Cr(CO)₄{C(OEt)}₂C₄H₂S] (6), [W(CO)₄{C(OEt)}₂C₄H₂S] (7) [Cr(CO)₄{C(OEt)}₂C₄S] (8) [W(CO)₄{C(OEt)}₂C₄S] (9). To a solution of tetrabromothiophene (0.40 g, 1.0 mmol) in 40 mL THF was cooled to -78°C and *n*-BuLi (1.25 mL of a 1.6 M solution in hexane, 2.0 mmol) was added. Within 5 min, metal hexacarbonyl, Cr(CO)₆ (0.44 g, 2 mmol) or W(CO)₆ (0.70 g, 2.0 mmol) was added and the solution was warmed to room temperature and reacted until all the metal carbonyl was converted. The solution was cooled to -78°C and a second portion of *n*-BuLi (1.25 mL, 2.0 mmol) was added and the reaction mixture was warmed to room temperature. The solvent was removed *in vacuo* and the residue dissolved in DCM. An excess [Et₃O][BF₄] (1.2 g, 6.3 mmol) was added at -35°C and the alkylation progress monitored by thin layer chromatography. After completion, the DCM was removed and the residue loaded onto a silica gel column and eluted with hexane. Three products separated and yielded [M(CO)₅{C(OEt)Bu}] (less

than 2%, W, Cr), **6** (0.16 g, 44% yield) or **7** (0.23 g, 46% yield) and the third product was the major compound of the reaction and contained two chelating biscarbene ligands, $[\{M(\text{CO})_4\{\text{C}(\text{OEt})\}_2\text{C}_4\text{S}\}]$ M = Cr **8**, W **9**).

8: Yield: 0.30 g (0.47 mmol, 47%), blue–black crystals. ^1H NMR (CDCl_3 , 500.139 MHz) δ : 4.84 (q, 7.1 Hz, 2H, C3(CH₂)), 4.76 (q, 7.1 Hz, 2H, C3(CH₂)), 1.58 (t, 6.9 Hz, 3H, C3(CH₃)), 1.56 (t, 6.9 Hz, 3H, C2(CH₃)). ^{13}C NMR (CDCl_3 , 125.75 MHz) δ : 316.5 (C3_{carb}), 301.7 (C2_{carb}), 245.5 ((Cr(CO)₄)_{trans}), 239.5 ((Cr(CO)₄)_{trans}), 226.0 ((Cr(CO)₄)_{cis}), 165.0 (C2), 151.3 (C3), 77.4 (C3(CH₂)), 76.4 (C2(CH₂)), 15.2, 14.3 (CH₃). IR (cm^{-1} , hexane, ν_{CO}): Cr(CO)₄: A₁⁽¹⁾ 2009 (m), A₁⁽²⁾ 1966 (s), B₁ 1946 (s), B₂ 1905 (m). Anal. Calcd. (%) for C₂₄H₂₀O₁₂SCr₂ (636.46 g/mol): C 45.29, H 3.17%. Found: C 45.41, H 3.28%.

9: Yield: 0.39 g (0.43 mmol, 43 %), blue–black crystals. ^1H NMR (CDCl_3 , 500.139 MHz) δ 4.58 (q, 7.2 Hz, 2H, C3(CH₂)), 4.54 (q, 7.1 Hz, 2H, C2(CH₂)), 1.62 (t, 7.1 Hz, 3H, C3(CH₃)), 1.61 (t, 7.2 Hz, 3H, C2(CH₃)). ^1H NMR (C_6D_6 , 500.139 MHz) δ 6.96 (d, 6.9 Hz, 1H, H5), 7.31 (d, 6.9 Hz, 1H, H4), 4.45 (q, 7.1 Hz, 2H, C3(CH₂)), 4.44 (q, 7.1 Hz, 2H, C2(CH₂)), 1.86 (t, 7.1 Hz, 3H, C3(CH₃)), 1.86 (t, 7.1 Hz, 3H, C2(CH₃)). ^{13}C NMR (C_6D_6 , 125.75 MHz) δ : 317.8 (C3_{carb}), 283.7 (C2_{carb}), 212.4 ((W(CO)₄)_{trans}), 209.1 ((W(CO)₄)_{trans}), 194.8 ((W(CO)₄)_{cis}), 165.4 (C3), 158.3 (C2), 81.2 (C3(CH₂)), 79.9 (C2(CH₂)), 14.8, 14.7 (CH₃). IR (cm^{-1} , hexane, ν_{CO}): M(CO)₄: A₁⁽¹⁾ 2017 (m), A₁⁽²⁾ 1961 (s), B₁ 1945 (s), B₂ 1897 (m). Anal. Calcd. (%) for C₂₄H₂₀O₁₂SW₂ (900.15 g/mol): C 32.08, H 2.24%. Found: C 32.39, H 2.36%.

Preparation of the chelated biscarbene complexes: [Cr(CO)₄{C(OEt)}₂C₆H₂S₂] (10**) [W(CO)₄{C(OEt)}₂C₆H₂S₂] (**11**), [Cr(CO)₄{C(OEt)}₂C₆H₁S₂{C(OEt)Cr(CO)₅] (**12**), [W(CO)₄{C(OEt)}₂C₆H₁S₂{C(OEt)W(CO)₅] (**13**), {[Cr(CO)₄{C(OEt)}₂C₆S₂] (**14**) [W(CO)₄{C(OEt)}₂C₆S₂] (**15**)** A solution of 4,4',5,5'-tetrabromothiopheno[2,3-*b*]thiophene (1.14 g, 2.5 mmol) in THF was cooled to -78°C and treated with 4.29 mL (6.0 mmol) *n*-BuLi. The reaction mixture almost immediately changed to yellow. Within five minutes the metal carbonyl Cr(CO)₆ (1.10 g, 5.0 mmol) or W(CO)₆ (1.76 g, 5.0 mmol) was added, and the solution was heated quickly to RT and stirred until all the metal carbonyl dissolved. A second portion of *n*-BuLi, 4.29 mL (6.0 mmol) was added at -78°C , after which the solution was heated to room temperature. The solvent was removed *in vacuo* and the residue dissolved in 10 mL of dichloromethane and cooled to -20°C . Alkylation was done with 4.50 g (23.7 mmol) of [Et₃O][BF₄] in DCM and the reaction mixture was allowed to rise to room temperature. The solvent was removed *in vacuo* and the reaction mixture wet loaded on a silica gel column. The products were separated using flash chromatography and gradient elution with hexane and DCM.

In addition to **12** and **14**, 0.05 g of **3** (0.075 mmol, 3%) and trace amounts of **10** were isolated for the reaction with chromium. The reaction with tungsten yielded **13** and **15**, along with 0.09 g of **4** (0.1 mmol, 4%) and 0.01 g (0.025 mmol, 1%) of **11**.

10: Yield: trace amounts, red solids. ^1H NMR (CDCl_3 , 300.13 MHz) δ : 7.45 (d, 5.3 Hz, 1H, H5'), 7.39 (d, 5.3 Hz, 1H, H4'), 4.84 (q, 7.1 Hz, 2H, C7(CH₂)), 4.73 (q, 7.1 Hz, 2H, C6(CH₂)), 1.62 (t, 7.1 Hz, 3H, C7(CH₃)), 1.62 (t, 7.1 Hz, 3H, C6(CH₃)). ^{13}C NMR (CDCl_3 , 75.468 MHz) not enough sample.

11: Yield: 0.01 g (0.025 mmol, 1%), red solids. ^1H NMR (CDCl_3 , 300.13 MHz) δ : 7.49 (d, 5.3 Hz, 1H, H5'), 7.45 (d, 5.3 Hz, 1H, H4'), 4.52 (q, 7.1 Hz, 2H, C7(CH₂)), 4.49 (q, 7.1 Hz, 2H, C6(CH₂)), 1.70 (t, 7.1 Hz, 3H, C7(CH₃)), 1.61 (t, 7.1 Hz, 3H, C6(CH₃)). ^{13}C NMR (CDCl_3 , 75.468 MHz) δ 289.3 (C7_{carb}), 281.8 (C6_{carb}), 220.4 and 220.2 ((W(CO)₄)_{trans}), 212.4 ((W(CO)₄)_{cis}), 171.4 (C5), 160.2 (C4), 136.6, n.o. (C3, C2), 130.5 (C5'), 121.9 (C4'), 79.8 (C7(CH₂)), 79.4 (C6(CH₂)), 14.8 (C7(CH₃)), 14.7 (C6(CH₃)). IR (cm^{-1} , hexane, ν_{CO}): M(CO)₄: A₁⁽¹⁾ 2028 (m), A₁⁽²⁾ 1960 (vs), B₁ 1959 (sh), B₂ 1894 (m). Calc C₁₆H₁₂O₆S₂W (547.96 g/mol) MS (m/z, intensity (%)); 606.91 (5%) [M+MF-H]⁻ (MF = methyl formate).

12: Yield: 0.38 g (0.6 mmol, 23 %), purple–black crystals. ^1H NMR (CDCl_3 , 300.13 MHz) δ : 8.61 (s, 1H, H4'), 5.20 (q, 7.0 Hz, 2H, C6'(CH₂)), 4.71 (q, 7.1 Hz, 2H, C7(CH₂)), 4.66 (q, 7.1 Hz, 2H, C6(CH₂)), 1.77 (t, 7.1 Hz, 3H, C6'(CH₃)), 1.69 (t, 7.0 Hz, 3H, C7(CH₃)), 1.59 (t, 7.1 Hz, 3H, C6(CH₃)). ^{13}C NMR (CDCl_3 , 75.468 MHz) δ : 315.1 (C6'carb), 314.9 (C7carb), 307.2 (C6carb), 243.8 and 243.5 ((Cr(CO)₄)_{trans}), 228.1 ((Cr(CO)₄)_{cis}), 223.0 ((Cr(CO)₅)_{trans}), 216.7 ((Cr(CO)₅)_{cis}), 158.6 (C5), 156.9 (C4), 135.9, 154.4 (C3, C2), 164.4 (C5'), 135.8 (C4'), 77.2 (C6'(CH₂)), 76.8 (C7(CH₂)), 76.2 (C6(CH₂)), 15.1 (C6'(CH₃)), 15.1 (C7(CH₃)), 15.0 (C6(CH₃)). IR (cm^{-1} , hexane, ν_{CO}): M(CO)₅: A₁⁽¹⁾ 2059 (m), B₁ 1989 (vw), A₁⁽²⁾ 1951 (sh), E 1951 (vs), M(CO)₄: A₁⁽¹⁾ 2021 (m), A₁⁽²⁾ 1968 (vs), B₁ 1964 (sh), B₂ 1903 (m). Calc. C₂₄H₁₆O₁₂S₂Cr₂ (663.89 g/mol) MS (m/z, intensity (%)); 662.88 (9%) [M–H][–].

13: Yield: 0.44 g (0.5 mmol, 19 %), purple–black crystals. ^1H NMR (CDCl_3 , 300.13 MHz) δ : 8.59 (s, 1H, H4'), 5.00 (q, 7.1 Hz, 2H, C6'(CH₂)), 4.44 (q, 7.1 Hz, 2H, C7(CH₂)), 4.43 (q, 7.1 Hz, 2H, C6(CH₂)), 1.78 (t, 7.1 Hz, 3H, C6'(CH₃)), 1.68 (t, 7.1 Hz, 3H, C7(CH₃)), 1.60 (t, 7.1 Hz, 3H, C6(CH₃)). ^{13}C NMR (CDCl_3 , 75.468 MHz) δ : 289.3 (C6'carb), 286.9 (C7carb), 279.8 (C6carb), 220.5 and 220.1 ((W(CO)₄)_{trans}), 212.4 ((W(CO)₄)_{cis}), 202.1 ((W(CO)₅)_{trans}), 197.2 ((W(CO)₅)_{cis}), 161.7 (C5), 160.8 (C4), 137.3, 155.0 (C3, C2), 171.3 (C5'), 136.7 (C4'), 80.1 (C6'(CH₂)), 79.6 (C7(CH₂)), 78.7 (C6(CH₂)), 14.9 (C6'(CH₃)), 14.8 (C7(CH₃)), 14.7 (C6(CH₃)). IR (cm^{-1} , hexane, ν_{CO}): M(CO)₅: A₁⁽¹⁾ 2066 (m), B₁ 1986 (vw), A₁⁽²⁾ 1947 (sh), E 1947 (vs), M(CO)₄: A₁⁽¹⁾ 2027 (m), A₁⁽²⁾ 1961 (vs), B₁ 1947 (sh), B₂ 1895 (m). Calc. C₂₄H₁₆O₁₂S₂W₂ (927.91 g/mol) MS (m/z, intensity (%)); 926.92 (3%) [M–H][–].

14: Yield: 0.71 g (1.0 mmol, 41 %), blue–black crystals. ^1H NMR (CDCl_3 , 300.13 MHz) δ : 4.73 (q, 7.1 Hz, 4H, C7(CH₂)), 4.70 (q, 7.1 Hz, 4H, C6(CH₂)), 1.61 (t, 7.1 Hz, 6H, C7(CH₃)), 1.54 (t, 7.1 Hz, 6H, C6(CH₃)). ^{13}C NMR (CDCl_3 , 75.468 MHz) δ : 319.5 (C7carb), 310.7 (C6carb), 242.3 and 239.4 ((Cr(CO)₄)_{trans}), 227.7 ((Cr(CO)₄)_{cis}), 164.1 (C5), 159.8 (C4), n.o. (C3, C2), 77.2 (C7(CH₂)), 76.4 (C6(CH₂)), 15.0 (C7(CH₃)), 14.8 (C6(CH₃)). IR (cm^{-1} , hexane, ν_{CO}): M(CO)₄: A₁⁽¹⁾ 2021 and 2009 (m), A₁⁽²⁾ 1955 (vs), B₁ 1945 (sh), B₂ 1888 (m). Calc. C₂₆H₂₀O₁₂S₂Cr₂ (691.92 g/mol) MS (m/z, intensity (%)); 690.90 (4%) [M–H][–].

15: Yield: 1.03 g (1.1 mmol, 43%), blue–black crystals. ^1H NMR (CDCl_3 , 400.13 MHz) δ : 4.49 (q, 7.1 Hz, 4H, C7(CH₂)), 4.43 (q, 7.1 Hz, 2H, C6(CH₂)), 1.61 (t, 7.1 Hz, 6H, C7(CH₃)), 1.54 (t, 7.1 Hz, 6H, C6(CH₃)). ^{13}C NMR (CDCl_3 , 100.613 MHz) δ : 293.8 (C7carb), 283.7 (C6carb), 219.5 and 217.2 ((W(CO)₄)_{trans}), 211.6 ((W(CO)₄)_{cis}), 170.0 (C5), 163.5 (C4), n.o., 155.0 (C3, C2), 79.8 (C7(CH₂)), 79.6 (C6(CH₂)), 14.7 (C7(CH₃)), 14.5 (C6(CH₃)). IR (cm^{-1} , hexane, ν_{CO}): M(CO)₄: A₁⁽¹⁾ 2029 and 2018 (m), A₁⁽²⁾ 1950 (vs), B₁ 1938 (sh), B₂ 1874 (m). Calc. C₂₆H₂₀O₁₂S₂W₂ (955.94 g/mol) MS (m/z, intensity (%)); 954.97 (28%) [M–H][–].

Conclusions

A series of novel Fischer multicarbene complexes could be synthesized by using deprotonation–, lithium–halogen exchange and stepwise lithiation reactions along with the removal of bromine by alkylating with excess triethyloxonium tetrafluoroborate. Examples of these are demonstrated by the preparation of complexes with monocarbene–, chelating biscarbene– and mixed metal biscarbene– ligands. Both the number of Fischer carbene moieties and different types of carbene units on a single thieno[2,3-*b*]thiophene backbone are without precedent in Fischer carbene complex chemistry. Blocking one side of a thiophene backbone by a fused second thiophene ring in a 2,3-*b* fashion has electronic and geometric consequences. The triscarbene complexes **12** and **13** are exceptional and the presence of three electronically different carbene carbons creates the opportunity for selective and diverse reactivity patterns. The formation of the analogous triscarbene complex of thiophene was not observed, which we ascribe to the absence of inter–ring conjugation in thieno[2,3-*b*]thiophene. Also unique in Fischer carbene chemistry is the fusion of four 5–membered rings with the two biscarbene chelate rings at the termini of the thieno[2,3-*b*]thiophene linker, affording a curved macromolecule that describes a semicircle. Solid state structures confirmed the stabilization of multicarbene complexes as a result of two carbene ligands being part of a chelate ring and a rigid planar linker between the metal carbonyl fragments. In spite of

steric congestion, **8** and **9** are stable in the solid state. Complexes **5**, **7**, **13** and **15** display intermolecular interactions and different packing phenomena, because of the different types of carbene ligands.

Associated Content

Crystallographic data (CIF files) for the reported structures have been deposited with the Cambridge Crystallographic Data Centre: **2** (CCDC 1401808), **4** (CCDC 1401809), **5** (CCDC 1401810), **7** (CCDC 1422363), **13** (CCDC 1401811) and **15** (CCDC 1401812). The data can be obtained free of charge from The Director, Cambridge Crystallographic Data Centre, 12 Union Road, Cambridge CB2 1EZ, UK, fax 44 1223 336 033, e-mail: deposit@ccdc.cam.ac.uk or via www.ccdc.cam.ac.uk/conts/retrieving.html.

Author information. simon.lotz@up.ac.za (SL); daniela.bezuidenhout@up.ac.za (DIB)

Acknowledgments

We are grateful for assistance by Mr. E. R. Palmer (NMR) and Dr. D. Koot (MS). This work was supported financially by the National Research Foundation (NRF) of South Africa with grants to SL (no. 73679 and 77079) and DIB (no. 87890 and 92521).

References

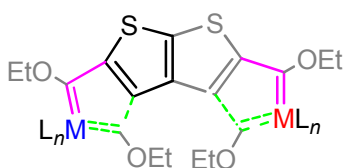
1. For reviews see: (a) H. G. Raubenheimer, *Dalton Trans.*, 2014, **43**, 16959–16973. (b) J. W. Herndon, *Coord. Chem. Rev.*, 2013, **257**, 2800–3003, and previous annual reviews. (c) *Metal Carbenes in Organic Synthesis, Top. Organomet. Chem.* (Ed.: K. H. Dötz), Vol. 13, Springer–Verlag, Berlin, Heidelberg, 2004.
2. (a) D. J. Nelson, *Eur. J. Inorg. Chem.* 2015, 2012–2027. (b) P. de Fremont, N. Marion and S. P. Nolan, *Coord. Chem. Rev.*, 2009, **253**, 862–892. (c) J. A. Mata, F. E. Hahn and E. Peris, *Chim. Sci.*, 2014, **5**, 1723–1732.
3. (a) E. O. Fischer, W. Röhl, U. Schubert and K. Ackermann, *Angew. Chem. Int. Ed. Engl.*, 1981, **20**, 611–612. (b) E. O. Fischer, W. Röhl, N. H. T. Huy and K. Ackermann, *Chem. Ber.*, 1982, **115**, 2951–2964. (c) K. Öfele, F. Dyckhoff and H. G. Krist, *Chem. Ber.*, 1993, **126**, 2573–2578. (d) N. H. T. Huy, E. O. Fischer, J. Riede, U. Thewalt and K. H. Dötz, *J. Organomet. Chem.*, 1984, **273**, C29–32.
4. N. H. T. Huy, C. Pascard, E. T. h. Dau and K. H. Dötz, *Organometallics* 1988, **7**, 590–592.
5. (a) N. A. van Jaarsveld, D. C. Liles and S. Lotz, *Dalton Trans.*, 2010, **39**, 5777–5779. (b) S. Lotz, N. A. van Jaarsveld, D. C. Liles, C. Crause, H. Görls and Y. M. Terblans, *Organometallics*, 2012, **31**, 5371–5383.
6. (a) J. Roncali, *Chem. Rev.*, 1992, **92**, 711–738. (b) *Handbook of Oligo- and Polythiophenes* (Ed. D. Fichou), Wiley–VCH, Weinheim, Germany 1999. (c) P. Bäuerle, *Oligothiophenes in Electronic Materials: The Oligomeric Approach*. (Ed. G. Wegner and K. Müllen), Wiley–VCH, Weinheim, 1998.
7. (a) W. Jiang, Y. Li and Z. Wang, *Chem. Soc. Rev.*, 2013, **42**, 6113–6127. (b) I. P. Perepichka, D. F. Perepichka, H. Meng and F. Wudl, *Adv. Mater.* 2005, **17**, 2281–2305. (c) J. Youn, P–Y. Huang, Y–W. Huang, M–c. chen, Y–J. Lin, H. Huang, R.P. Ortiz, C. Stern, M–C. Chung, C–Y Feng, L–H. Chen, A. Facchetti and T. J. Marks, *Adv. Funct. Mater.*, 2012, **27**, 48–60.

8. (a) R. J. Angelici, *Coord. Chem. Rev.*, 1990, **105**, 61–76. (b) T. B. Rauchfuss, *Prog. Inorg. Chem.*, 1991, **39**, 259–329. (c) S. Lotz, P. H. van Rooyen and R. Meyer, *Adv. Organomet. Chem.*, 1995, **37**, 219–320. (d) S. Lotz, C. Crause, A. J. Olivier, D. C. Liles, H. Görls, M. Landman and D. I. Bezuidenhout, *Dalton Trans.* 2009, 697–710.
9. (a) M. Landman, H. Görls and S. Lotz, *J. Organomet. Chem.*, 2001, **617–618**, 280–287. (b) M. Landman, H. Görls and S. Lotz, *Eur. J. Inorg. Chem.*, 2001, 233–238. (c) M. Landman, H. Görls and S. Lotz, *Z. Anorg. Allg. Chem.*, 2002, **628**, 2037–2043.
10. (a) D. I. Bezuidenhout, S. Lotz, D. C. Liles and B. van der Westhuizen, *Coord. Chem. Rev.*, 2012, **256**, 479–524. (b) M. P. López-Alberca, M. J. Mancheño, I. Fernández, M. Gómez-Gallego, M. A. Sierra, C. Hemmert and H. Gornitzka. *Eur. J. Inorg. Chem.* 2011, 842–849. (c) C. Hartbaum, G. Roth and H. Fischer. *Eur. J. Inorg. Chem.* 1998, 191–202. (d) L. Quast, M. Nieger and K. H. Dötz. *Organometallics* 2000, **19**, 2179–2183.
11. T. Otsubo, Y. Kono, N. Hozo, H. Miyamoto, Y. Aso, F. Ogura, T. Tanaka and M. Sawada, *Bull. Chem. Soc. Jpn.*, 1993, **66**, 2033–2041.
12. V. Fiandanese, D. Bottalico, G. Marchese and A. Punzi, *Tetrahedron*, 2006, **62**, 5126–5132
13. C. Crause, H. Görls and S. Lotz, *Dalton Trans.*, 2005, 1649–1657.
14. J. Barluenga, A. A. Trabanco, I. Pérez-Sánchez, R. de la Campa, J. Flórez, S. García-Granda, A. Aguirre, *Chem. Eur. J.*, 2008, **14**, 5401–5404.
15. P. Fournari and P. Meunier, *Bull. Soc. Chim. Fr.*, 1974, **3–4**, 583–586.
16. (a) F. W. Evans, R. J. Fox and M. Szwarc, *J. Am. Chem. Soc.*, 1960, **82**, 6414–6415; (b) M. J. Diem, D. F. Burow and J. L. Fry, *J. Org. Chem.*, 1977, **42**, 1801–1802.
17. S. Gronowitz and B. Persson. *Acta Chem. Scand.* 1967, **21**, 812–813.
18. M Hesse, H. Meier and B. Zeeh, *Spektroskopische Methoden in der organischen Chemie*, Georg Thieme Verlag: Stuttgart, 1984, 153.
19. D. M. Adams. *Metal–Ligand and Related Vibrations*; Edward Arnold Publishers Ltd: London, 1967, 98–101.
20. C. P. Brock and J. D. Dunitz, *Chem. Mater.*, 1994, **6**, 1118–1127.
21. L. Brandsma, S. F. Vasilevsky and H. D. Verkruijsse, *Application of transition metal catalysts in organic synthesis*, Springer: Berlin, 1998, 25–26.
22. H. Meerwein, *Org. Synth.*, 1966, **46**, 113–115.
23. APEX2 (including SAINT and SADABS); BrukerAXS Inc., Madison, WI, 2015.
24. G. M. Sheldrick, *Acta Crystallogr.* 2015, **A71**, 3–8.

25. G. M. Sheldrick, *Acta Crystallogr.* 2015, **C71**, 3–8.

TOC entry

The syntheses, spectroscopic and structural properties of new mono- to tetracarbene mono- and dinuclear Fischer carbene complexes of (condensed) thiophene.



$ML_n = M(CO)_{4/5}$, $M = Cr$ and / or W